

pubs.acs.org/Macromolecules Article

Strong Polyelectrolyte Brushes via Alternating Copolymers of Styrene and Maleimides: Synthesis, Properties, and Stability

Gozde Aktas Eken and Christopher K. Ober*



Cite This: Macromolecules 2022, 55, 5291-5300



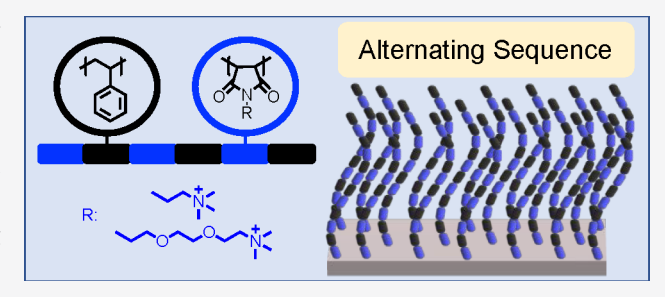
ACCESS I

Metrics & More

Article Recommendations

Supporting Information

ABSTRACT: Polyelectrolyte brushes are of great interest for various applications from smart actuators to fouling resistant surfaces. Strong stretching due to proximity and Coulombic repulsion of the neighboring chains is a key to their function, which creates tension along the polymer chains and leads to degrafting of polymer brushes from the surfaces. A promising approach to lower the tension along the backbone is to reduce the number of charged units. Herein, we report a series of strong polyelectrolyte brushes with precisely controlled architectures, based on the alternating copolymers of styrene and N-substituted



maleimides. Alternating copolymerization is employed to ensure the homogeneous distribution of charged units and dilute the charge density. Tailor-made maleimide monomers bearing hydrocarbon spacers with cationic groups are copolymerized with styrene via surface-initiated Activators ReGenerated by Electron Transfer Atom Transfer Radical Polymerization (SI-ARGET ATRP). Swelling behavior of the brushes is investigated as a function of molecular weight and pH. In solution atomic force microscopy (AFM) analyses and water contact angle measurements revealed that it is possible to obtain PEBs with good hydration properties, by combining hydrophobic and ionic units in an alternating sequence. Results also proved that the spacers play an important role in swelling behavior and wettability of brushes. Stability of the brushes is evaluated through incubation tests, and AFM is used to follow the changes in thickness and surface morphology. Brushes retained more than 80% of their original height after 3 weeks in buffer solutions. This study provides a novel approach to design PEBs with enhanced stability and adjustable macromolecular architecture.

INTRODUCTION

Polymer brushes (PBs) consist of polymer chains that are densely tethered to a surface by one end. Surface modification through polymer brushes has become a powerful tool due to the high degree of synthetic flexibility on various substrates including metal, glass, and polymer surfaces.^{2–4} PBs enable the obtainment of functional coatings with well-controlled composition, architecture, and thickness. Polyelectrolyte brushes (PEBs), which contain charged groups in their repeating units, constitute an important class of PBs.8 They exhibit distinctive properties due to the repulsive electrostatic and steric interactions; those can be adjusted by counterions, pH, salt concentration, and solvent quality. 9-11 Many applications have been described for PEBs including artificial joints, 12 enzyme immobilization supports, 13,14 smart actuators, 15,16 and responsive interfaces. 17 They have been widely used to modify surface properties such as fouling resistance, 18,19 wettability, 20,21 friction, 22,23 and adhesion. 24 There is a growing interest in applications of polymer brushes since these covalently tethered polymer films offer chemical and mechanical robustness. However, a number of studies proved the instability of PBs under certain conditions resulting with degrafting of polymer brushes from the surfaces.²⁵ Degrafting is proposed to be a mechanochemical process, which proceeds through hydrolytic cleavage of labile bonds in the substratepolymer interface, assisted with strong stretching.²⁶⁻³⁰ Polyelectrolyte brushes are subjected to stronger tension compared to their neutral peers, because of additional tension generated by electrostatic repulsion and osmotic pressure. Thus, they exhibit faster degrafting kinetics in a dense grafting regime.

To the date, the stability of PEBs has been investigated as a function of intrinsic and extrinsic parameters such as grafting density, degree of charging, molecular weight, confinement, solvent quality, and ionic strength. 31,32 Ko and Genzer studied degrafting of weak and strong polycationic brushes with varying molecular weights, charge degrees, and grafting densities,³³ where they reported that the degrafting increases with the degree of quaternization degree, molecular weight, and grafting density. Menzel et al. explored the stability of patterned and nonpatterned cationic brushes from the perspective of kinetic and thermodynamic effects.³⁴ Galvin

Received: March 29, 2022 Revised: June 14, 2022 Published: June 28, 2022





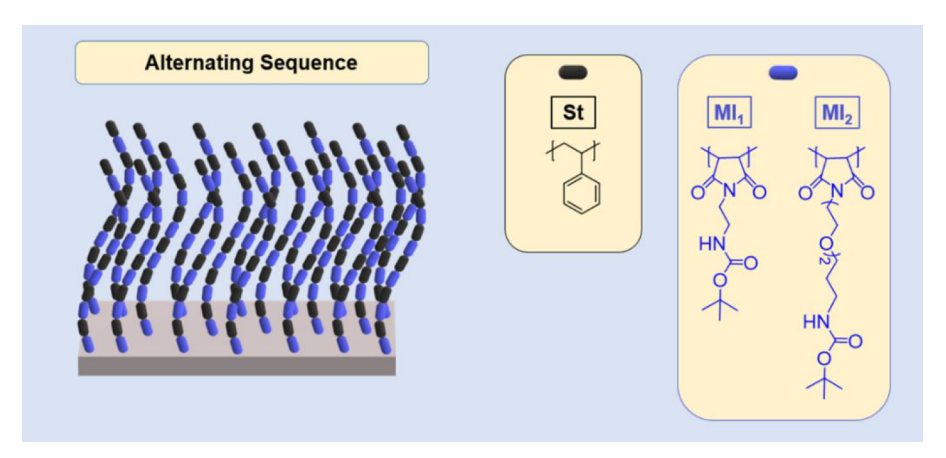


Figure 1. Schematic illustration of brushes with alternating sequence and monomers used to build charged and neutral segments.

and co-workers examined degrafting of weak polyanionic brushes with a range of grafting densities which are prepared from analogous ester and amide-bearing ATRP initiators. They proved that the presence of labile groups that are prone to hydrolysis contributes to the detachment of chains beside other parameters such as grafting density and protonation degree.³⁵ Similar results were reported by Ataman and Klok, where they investigated the stability of hydrophilic brushes synthesized through various ATRP initiators.³⁶ Several strategies have been developed to enhance the stability of PEBs, including copolymerization. Introduction of hydrophobic-neutral blocks between charged segments and the substrate through block copolymerization has been widely employed^{28,37,38} to create a hydrophobic shielding layer for the labile bonds and to reduce the tension at the polymersubstrate interface by hydrophobic spacers. However, weak points can be still introduced along the polymer chain where charged groups are direct neighbors. A better understanding of the effects of charge placement and charge density along the backbone and how those affect the mechanochemical stresses is required to design stable polymer brushes.

In this study, a novel approach is adopted; alternating copolymerization is employed to dilute the charge density along the backbone. A series of strong cationic PEBs with an alternating sequence of neutral and charged units are prepared and investigated to understand the effects of charge spacing and placement on swelling behavior and stability. PEBs are synthesized through surface-initiated Activators ReGenerated by Electron Transfer Atom Transfer Radical Polymerization (SI-ARGET ATRP) of styrene (electron-donor monomer) and N-substituted maleimides (strong electron-acceptor monomers). Cross-propagation of comonomers enabled distribution of the charges along the backbone uniformly and thus reduced charge density, 39,40 where the design of N-substituted maleimides with pendant chains bearing the quaternary ammonium groups were allowed to control the distance between the charged groups and the backbone. Brushes were grown from planar silicon surfaces with different film thicknesses then evaluated in buffer solutions with varying pH to provide a better understanding of the relationship between the macromolecular architecture and brush performance. To the best of our knowledge, effects of charge spacing and periodicity have not been systematically addressed yet.

EXPERIMENTAL SECTION

Materials. Maleic anhydride, di-tert-butyl dicarbonate, magnesium sulfate (MgSO₄), and sodium chloride (NaCl) were obtained from BTC. Acetone-d₆, chloroform-d (CDCl₃), 1,2-diaminoethane, 2,2'-(ethylenedioxy)bis(ethylamine), ethyl acetate, sodium acetate (NaAc), acetic anhydride, ethyl-2-bromoisobutyrate (EBiB), copper-(II) bromide (CuBr₂), tris[2-(dimethylamino)ethyl]amine (Me₆TREN), N,N-dimethylformamide (DMF), trimethylamine, 20 α bromoisobutyryl bromide (BIBB), ethanol (EtOH), dichloromethane (DCM), (3-aminopropyl)triethoxysilane (APTES), trifluoroacetic acid (TFA), (2-(methacryloyloxy)ethyl) trimethylammonium chloride (METAC), and styrene (St) were purchased from Sigma-Aldrich. L-Ascorbic acid was obtained from Fisher Scientific. Styrene was passed through an inhibitor removal column (Aldrich) before polymerization; others were used as received. A RiOs 3 Water Purification System was used to obtain deionized water (DIW). Silicon wafers (boron-doped, (100) orientation) were purchased from Pure Wafer.

Synthesis of N-Substituted Maleimides. N-substituted maleimides were synthesized through the reaction of maleic anhydride with mono-t-BOC protected diamine derivatives leading to maleamic acid intermediates, which are subsequently cyclized into the corresponding maleimides. Mono-t-BOC protected diamines that act as spacers and enable the separation of charged units from the backbone were prepared through the reaction of 1,2-diaminoethane and 2,2'-(ethylenedioxy)bis(ethylamine) with di-tert-butyl dicarbonate in 1,4-dioxane (6:1 molar excess of diamine to di-tert-butyl dicarbonate at 25 °C). A small amount of the bis-protected diamines was separated from the products by using their water insolubility. After evaporation of dioxane, the product was dispersed in 50 mL of DIW and insoluble bis compounds were removed by filtration. Watersoluble monoprotected diamines then were collected through extraction from the aqueous phase with DCM. The organic phase was dried over MgSO₄, and mono-t-BOC protected diamines were obtained after filtration of the drying agent and evaporation of the

Then, equimolar amounts of maleic anhydride and mono-t-BOC protected diamines were reacted in ethyl acetate that resulted in maleamic acid intermediates. The product, N-2-[(t-Boc)amino]ethyl maleamic acid, precipitated as a white solid and was recovered by vacuum filtration, washed with ethyl acetate, and dried, where N-(8-[(t-Boc)amino]-3,6-dioxaoctyl maleamic acid was obtained as a colorless oil and used in the next step without purification after characterization. For cyclization, maleamic acid intermediates were mixed with 0.3 mol equiv of anhydrous sodium acetate and 5.5 mol equiv of acetic anhydride. Then, the mixture was heated to 55 °C, and the reaction was monitored via 1 H NMR. Products were collected after 24 h and purified as described in the following. N-(2-[(t-Boc)amino]ethyl maleimide was obtained through precipitation, as a light brown powder with 80% yield. The reaction mixture precipitated

Scheme 1. Composition, Synthesis, and Modification of Poly(styrene-alt-N-maleimide) Brushes ([MI]/[St]/[EBiB]/[CuBr₂]/ [Me₆TREN]/[L-Ascorbic Acid] = 250/250/1/0.05/0.5/1.5)

in ice-cold DIW; the product was recovered by vacuum filtration and washed with cold DIW. However, N-(8-[(t-Boc)amino]-3,6-dioxaoctyl maleimide was obtained as pale yellow viscous oil through column chromatography (1:9 hexane/ethyl acetate) with 68% yield. Monomers were stored at -18 °C with desiccants.

Preparation of Polymer Brushes. Substrates with a surface immobilized ATRP initiator with an amide linker were prepared and characterized as described below. Silicon wafers were cut into 1.5×2 cm² pieces and sonicated in acetone for 10 min and then dried under a nitrogen flow. Then, the substrates were exposed to oxygen plasma for 45 min. After plasma treatment, they were immersed in a solution of APTES 4% (v/v) in ethanol for 1 h and dried under N_2 and then baked for 30 min at 120 °C. APTES treated wafers were immersed in a solution of BIBB (3 mmol) and TEA (3 mmol) in 15 mL of DCM for 24 h in an inert atmosphere. Wafers were removed from the solution, washed, and then stored in a desiccator.

Poly(styrene-alt-N-maleimide) brushes were synthesized through SI-ARGET ATRP from initiator-deposited silicon substrates, which were prepared with a multifunctional silanization agent, and an amide-

based ATRP initiator, to enhance the stability at the polymer/ substrate interface and minimize the effect of initiator/linker groups for a better comparison. Two series of samples (Figure 1) were prepared with different maleimides, which contain ethylene- and oligo(ethylene oxide)-based spacers; in each set there are four samples with varying thickness. Polymerization conditions were optimized through preliminary studies.

Polymerizations were carried out in the presence of sacrificial initiators with L-ascorbic acid as the reducing agent under given conditions of [MI]/[St]/[EBiB]/[CuBr $_2$]/[Me $_6$ TREN]/[L-ascorbic acid] = 250/250/1/0.05/0.5/1.5 in 4 mL of DMF at 110 °C. Samples were taken at certain time intervals, and free polymers were analyzed by $^1\mathrm{H}$ NMR spectroscopy and gel permeation chromatography (GPC, based on PS standards) to determine the composition and molecular weight of free polymers. After a certain time, substrates were removed from the reaction mixture, rinsed with DMF, and sonicated in THF to remove the physically adsorbed free polymers and dried under a nitrogen flow. Then, the substrates were analyzed via AFM, XPS, and goniometer.

Quaternization of poly(styrene-alt-N-maleimide) brushes was carried out after deprotection of t-BOC groups by immersing brushes in TFA/DCM (1:1 v/v) solution for 24 h. After deprotection, substrates were removed from the solution; washed with DCM, absolute ethanol, and Milli-Q water; and then dried under vacuum. Brushes were quaternized according to a previously reported procedure, which involves direct alkylation of primary amines in the presence of a sterically hindered organic base and an alkylating agent. Substrates immersed in a solution of tributylamine in DMF then methyl iodide were gradually added and the reaction proceeded for 72 h at 40 °C. Quaternized brushes were rinsed with DMF and ethanol with further sonication in ethanol for 5 min then dried under a vacuum at 40 °C for 24 h. Contact angle measurements and AFM and XPS analyses were performed on each sample.

To prepare the control series, polystyrene brushes were synthesized under identical conditions, and poly((2-(methacryloyloxy)ethyl) trimethylammonium chloride) (PMETAC) brushes were synthesized according to previously reported procedures. 42,43

Characterization. Molecular weight (M_n) and dispersity (D) of the free polymers were measured with an Agilent 1200 gel permeation chromatography (GPC) instrument using three PSS SDV columns (with molecular weight ranges of 1000–10 000 and 1000–1 210 000 g mol^{-1}) with a refractive index detector at 35 °C. THF was used as an eluent with a flow rate of 1.0 mL min^{-1} , based on PS standards. $^{1}\mathrm{H}$ NMR spectra of N-substituted maleimides and free polymers were recorded on a Varian Inova 500 spectrometer operating at 500 MHz at room temperature.

AFM measurements were conducted using an Oxford Instruments Cypher ES atomic force microscope equipped with an environmental scanner. Silicon tips (Oxford Instruments) with a resonance frequency of 300 kHz and a 26 N/m spring constant were used for the dry state, while the tips with a 70 kHz frequency and a 2 N/m spring constant were used for in-fluid analyses. The dry and wet thickness of brushes was measured through step-height measurements by AFM. To measure brush thickness, samples were carefully scratched with a razor blade, and AFM height images were taken at the boundary between the scratched and nonscratched regions. Imaging was conducted in tapping mode, and the thickness of each sample was measured in three different regions. To determine the swelling ratio, samples were incubated in buffer solutions and DIW for 2 h to equilibrate, then the wet thickness of swollen brushes was measured.

X-ray photoelectron spectroscopy (XPS) analyses were conducted using Scienta Omicron ESCA 2SR XPS equipped with a monochromatic Al K α high power X-ray source operating at a power of 150 W with an emission current of 12.5 mA. The base pressure in the spectrometer was around 10^{-8} mbar. Survey spectra (5 scans) were collected with a pass energy of 200 eV and a step size of 1 eV, and high resolution (10 scans) ones were collected with a pass energy of 50 eV and a step size of 0.05 eV. Casa XPS software was used for data processing including fitting.

Water contact angle (WCA) measurements were performed with an Attension Theta Lite goniometer using the sessile drop method; data were collected for a 10 s period within 60 s. The average of results was obtained from repeating measurements.

Degrafting Studies. Quaternized poly(styrene-*alt-N*-maleimide) brushes, PMETAC, and PS brushes as control groups were incubated in buffer solutions with at pH 3, 7, and 10, with 50 mM ionic strength. Samples stored at room temperature in sealed vials and periodic measurements were conducted via AFM at given time intervals, to determine the changes in film thickness and surface topography. Samples were rinsed with DI water and dried under a vacuum before characterizations.

■ RESULTS AND DISCUSSION

Mono-t-BOC protected diamines and N-substituted maleimides N-(2-[(t-Boc)amino]ethyl maleimide (MI₁) and N-(8-[(t-Boc)amino]-3,6-dioxaoctyl maleimide (MI₂) (Figure 1) are obtained in high yields, and 1H NMR spectra are provided in Figures S1–S4. Immobilization of the ATRP initiator was

confirmed by XPS analysis (Figure S5a) and WCA measurements (77.28 \pm 1.62°; Figure S6). The XPS spectrum shows the characteristic peaks of APTES-BIBB, which were observed at 533.9 (O 1s), 400.9 (N 1s), 285 (C 1s), and 71.9 (Br 3d) beside the 99.5 (Si 2s) eV (Figure S5a). Scheme 1 presents the route that is followed to synthesize and modify the brushes. Targeted brushes were prepared in three steps: (1) SI ARGET-ATRP of styrene and N-substituted maleimides (MI₁, MI₂) with t-BOC protected amine groups, (2) deprotection via TFA treatment, and (3) quaternization with an excess of methyl iodide. Two series of brushes, series A and B (Scheme 1), are prepared with MI₁ and MI₂ (Figure 1) and varying thicknesses from 9.5 to 50.4 nm and 5.5 to 48.8 nm, respectively. Composition and the dry thickness of brushes are summarized in Table 1.

Table 1. Composition and Dry Thickness of the Brushes

sample ID	monomer	dry thickness (nm)
S_1	MI_1	9.5 ± 0.2
S_2	\mathbf{MI}_1	14 ± 0.5
S_3	\mathbf{MI}_1	25.1 ± 0.3
S_4	\mathbf{MI}_1	50.4 ± 1.7
S_5	MI_2	5.5 ± 0.1
S_6	MI_2	12.4 ± 0.7
S_7	MI_2	18.6 ± 0.5
S_8	MI_2	48.8 ± 1.5

The MW gradient samples were prepared through kinetic studies for both series. Free polymers enabled the use of solution techniques such as ¹H NMR and GPC to analyze the composition and molecular weight. The resultant free polymers displayed unimodal GPC elugrams with molecular weight distributions [D: 1.3-1.6]. The correlation between the molecular weight (M_n) of free polymers and dry thickness of the brushes, determined via AFM, is represented in Figure 2a and b. A linear relationship is observed for series A where it is slightly deviated from the linear region for series B, most likely due to the bulkier structure of the monomer combined with the hydrophilicity that might affect the polymerization kinetics on the surface. Molecular weight of the surface tethered polymers is expected to be lower than the free polymers as a result of local viscosity and restricted mobility. 44 Therefore, the data have been used as an indicator of polymerization kinetics and composition of tethered polymers. The composition of the copolymers was determined through ¹H NMR by comparing the integrations of aromatic protons of styrene (6.5-7.5 ppm)to the protons of *tert*-butyl groups (1.45 ppm) or methine and methylene groups of maleimides (Equation S1). Representative NMR spectra are given in Figures S7 and S8. Composition analyses revealed that both copolymers are slightly rich in styrene, with a ratio of [St]/[MI] = 58:42, due to the bulky structure and electron-donating nature of substituted alkyl chains in the maleimide structure. It is known that the nature of substitutes is important, and the substituents enhancing the difference between electron densities of (co)monomers are more effective at obtaining precise alternating sequences. 45,46 The resulting copolymers did not display strictly defined alternating sequences, but they exhibited a predefined distribution of ionic groups along the polymer backbone.

Synthesis of the poly(styrene-alt-N-maleimide) brushes is confirmed with XPS analyses. A representative XPS survey spectrum of S_7 (Table 1) brushes is shown in Figure 3a. In

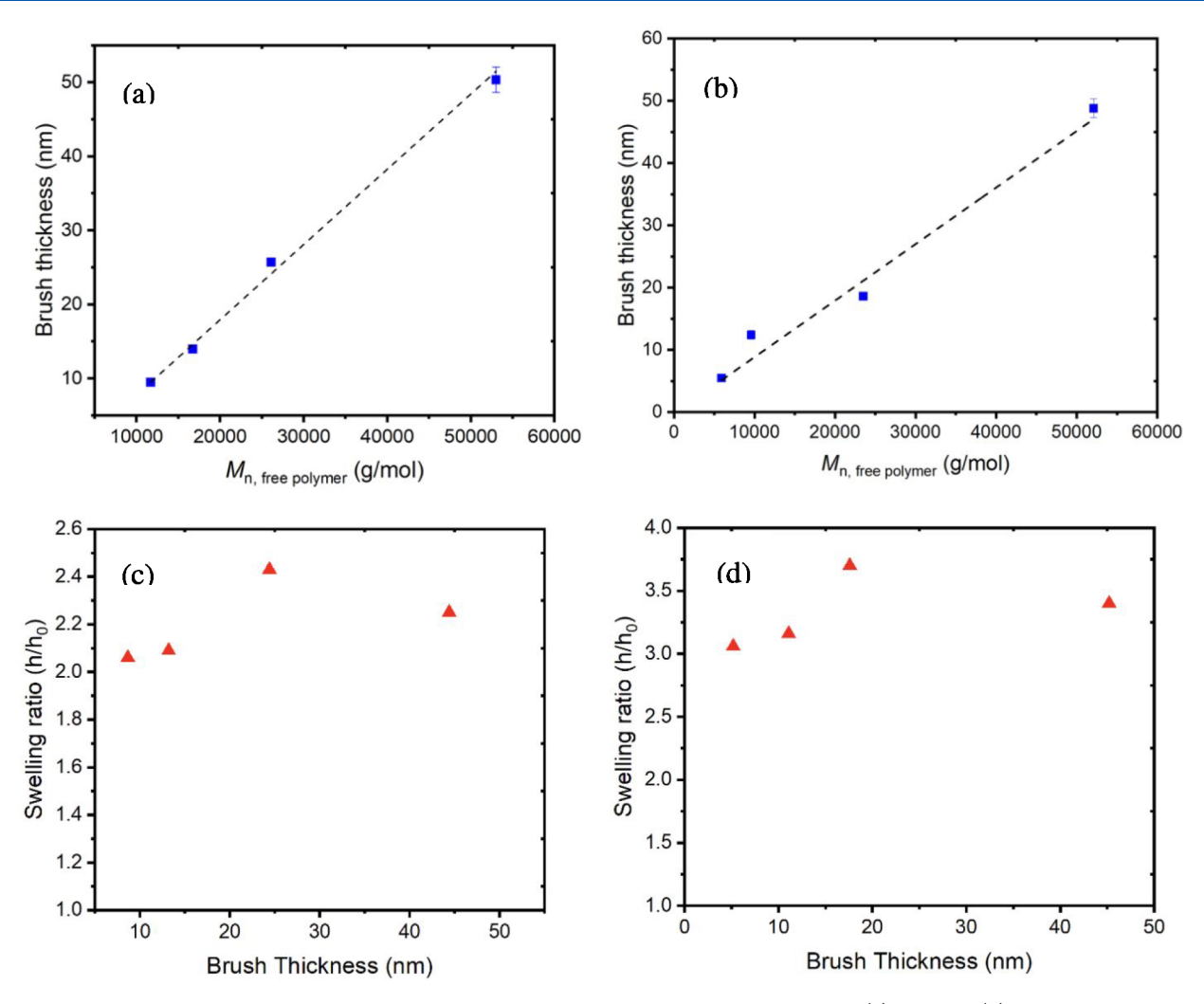


Figure 2. Relationship between the dry brush thickness measured by AFM and M_n of free polymers: (a) series A, (b) series B. Swelling ratio of quaternized brushes with different dry thickness in DIW: (c) series A, (d) series B.

addition to the peaks expected for poly(styrene-alt-Nmaleimide) brushes, disappearance of Si (2s, 2p) peaks also indicates brush growth and uniform surface coverage. Quaternization of the brushes was performed using various methyl iodides through the Menschutkin reaction in DMF, after deprotection. The appearance of iodine peaks in survey spectra of the brushes after confirmed quaternization is shown in Figure S5b. The degree of quaternization (DQ) was determined using the high-resolution spectra of N 1s. Figure 3b and 3c show deconvoluted core level peaks of N 1s before and after quaternization. Before deprotection, a broad peak around 401.6 eV was observed arising from the amide and imide nitrogens. 47,48 Quaternized samples exhibited two nitrogen peaks at 401.8 and 403.8 eV, assigned to the neutral (N^0) nitrogen atoms and quarternary ammonium groups (N^+) in the brush layer. 49,50 DQ was determined via peak-fitting and varied between 62 and 64% (Figure S9). Reaction times extended up to 1 week to achieve higher quaternization degrees. However, the degree of quaternization remained stable at 64%, most likely due to steric hindrance. Brushes displayed similar morphologies, with a dense, uniform polymer coating after quaternization (Figure S10).

Swelling behavior of the brushes with varying molecular weight was investigated for both series via in solution AFM analyses. Brushes were equilibrated in DIW for 2 h prior to the

measurements, and the swelling behavior was evaluated using the swelling ratio (h/h_0) , which is the ratio of swollen brush thickness (h) to dry brush thickness (h_0) . The thickness determined after quaternization is considered the initial dry thickness to calculate swelling ratio and height changes after stability tests. Swelling ratios determined through step height measurements are presented in Figure 2d and c. Brushes displayed swelling ratios close to the reported values in the literature for strong cationic brushes that are found between 2.06 and 2.43 for series A and 3.1 and 3.7 for series B. 11,33 Brushes in series B exhibited higher swelling ratios due to the contribution of oligo(ethylene oxide) spacers to the total hydrophilicity (Figure 4b). Swelling ratios varied with molecular weight, but no correlation was observed. Variations in swelling ratios can be explained by the dispersity of the brushes which affects the local stress and lateral pressure.²⁷ Results indicate that the hydrophobicity of the neutral units (styrene) can be surpassed through the combined effect of hydrophilic spacers and ionic groups, and the driving force created by these interactions is enough to create a 2- to 3.7fold increase in brush height. Strong swelling is one of the most critical factors that builds up the tension along the polymer backbone besides the steric and Coulombic interactions; thus the samples which exhibited the highest swelling ratios were

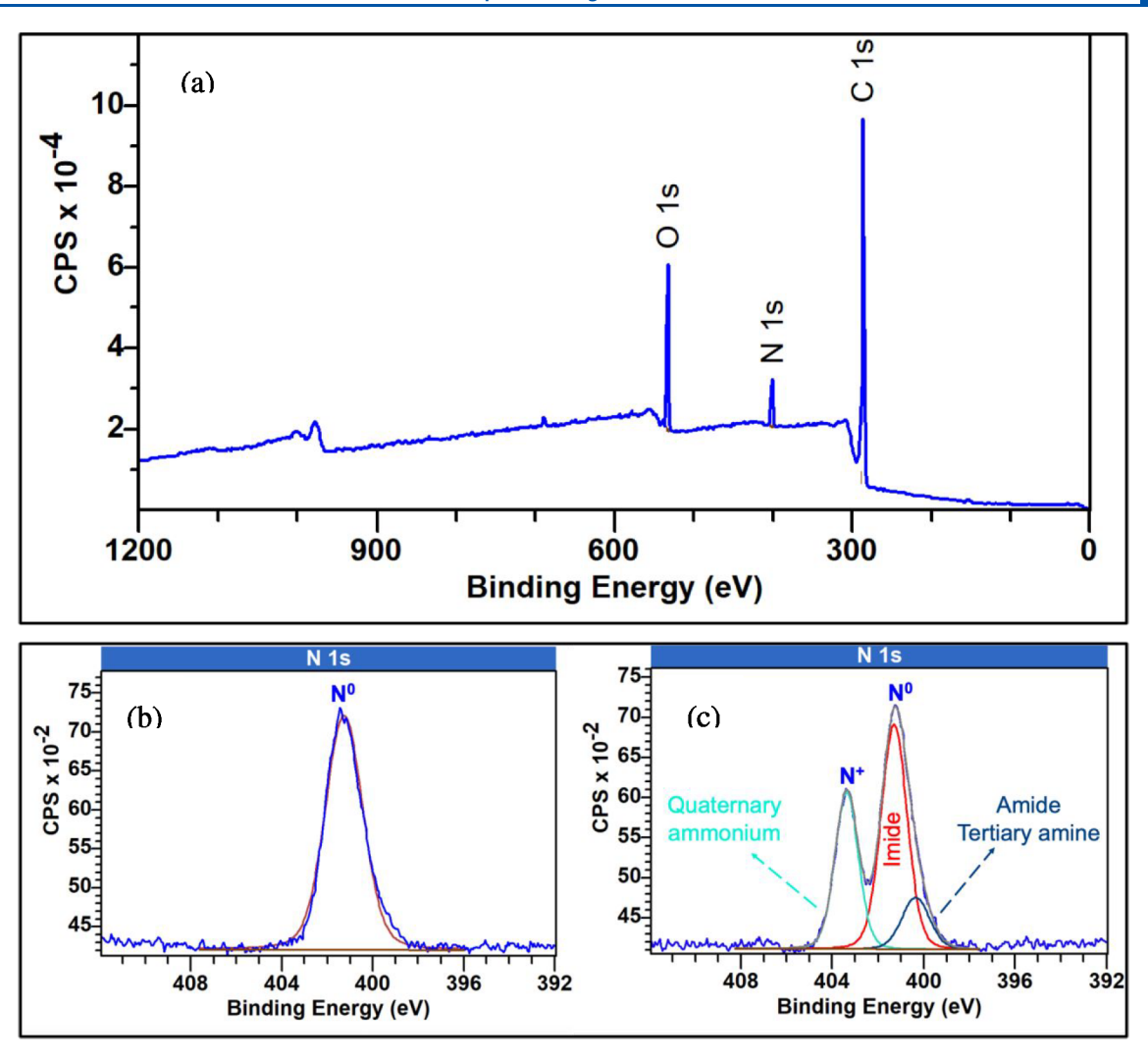


Figure 3. (a) XPS survey spectra of brushes $(S_7 h_0: 17.6 nm)$, (b) high resolution N 1s spectra of S_7 before deprotection, (c) after quaternization (fitting curve is gray).

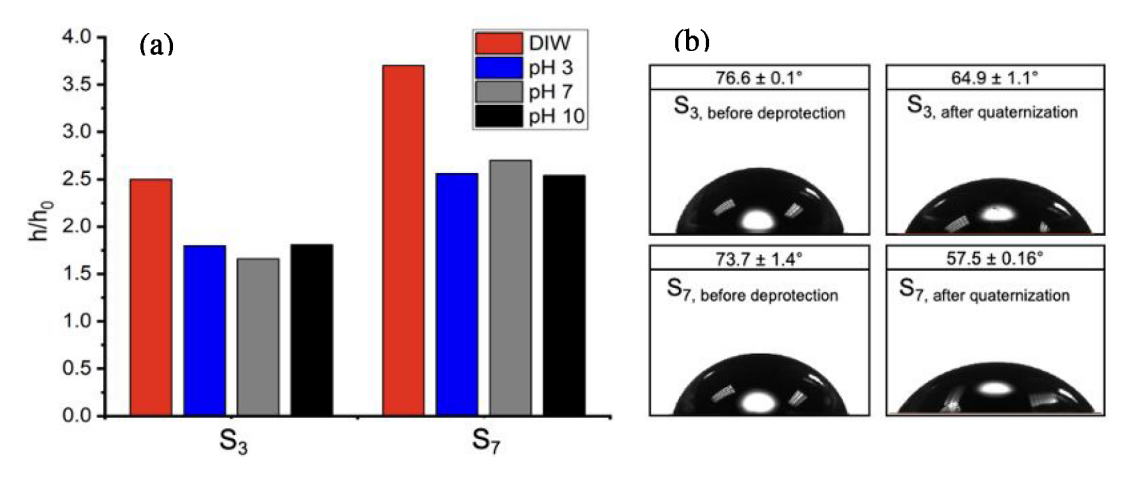


Figure 4. (a) Swelling ratio of brushes, S_3 and S_7 (Table 1), in DIW and buffer solutions with variable pH. (b) WCA of samples before (left) and after quaternization (right).

selected from each series $(S_3 \text{ and } S_7)$ for further characterizations and stability studies.^{35,38}

To explore the pH response of the quaternized brushes, in solution AFM analyses were conducted in buffer solutions for selected samples, S_3 and S_7 . Samples were incubated in

phosphate buffers at pH 3, 7, and 10, which contain 50 mM NaCl, and after 2 h of incubation the swollen brush heights measured at three different points and average values are reported. Dry state and in fluid AFM images captured in buffer solutions (height and phase) are shown in Figure 5. The root-

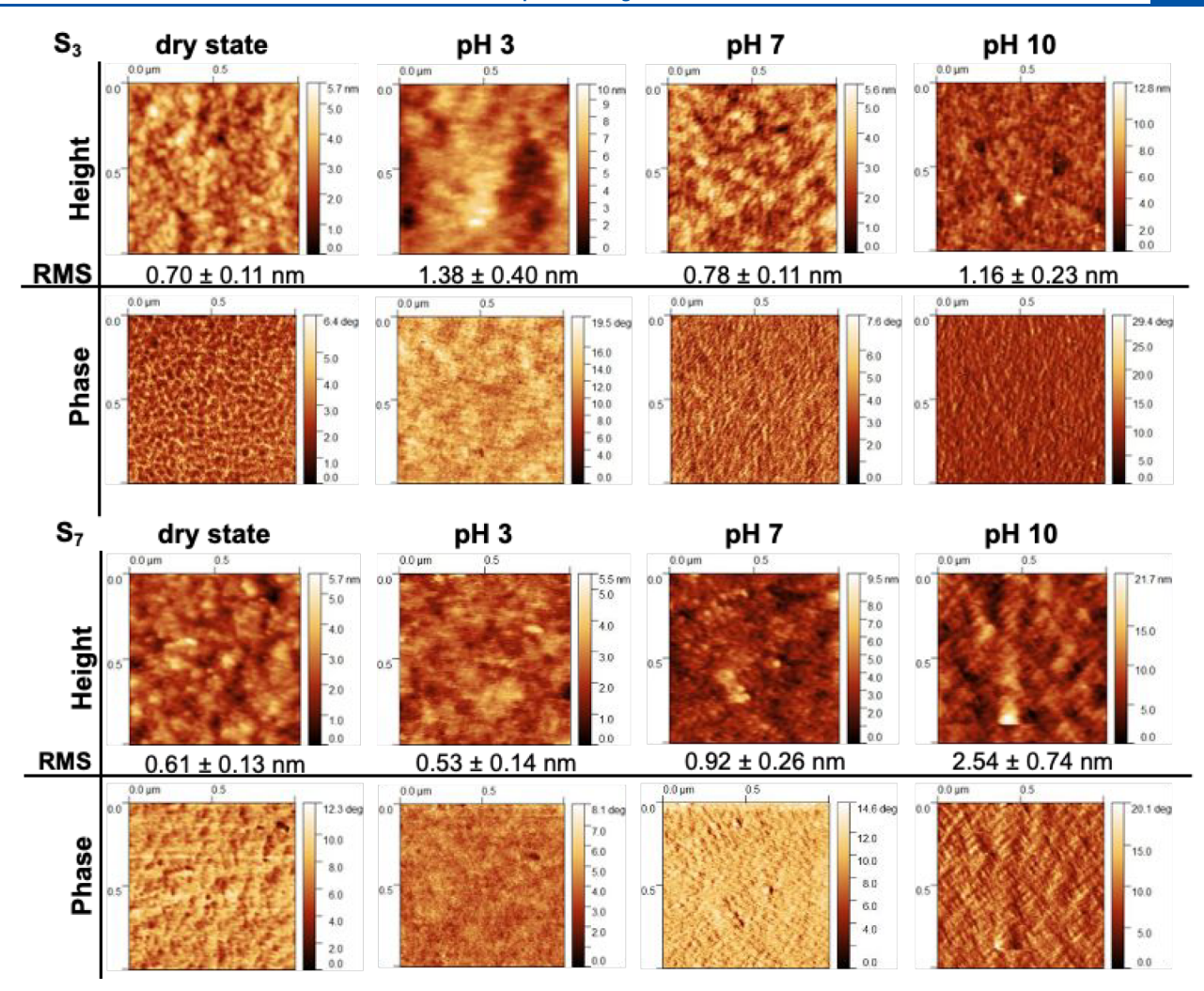


Figure 5. Dry state and in fluid AFM tapping-mode height and phase images of S_3 (top) and S_7 (bottom; 1 μ m × 1 μ m).

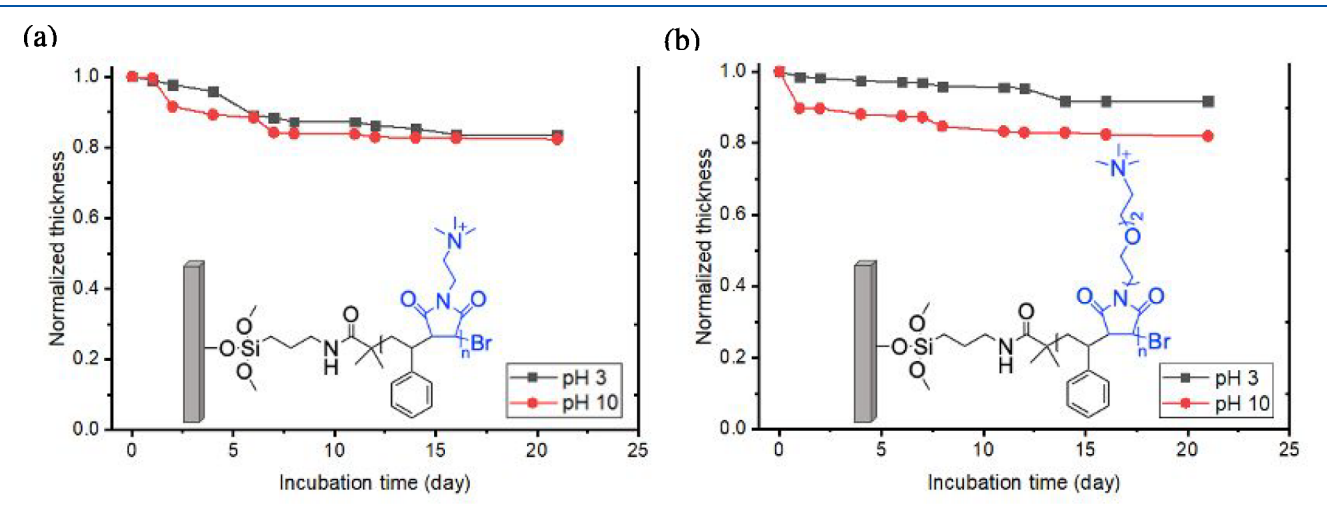


Figure 6. Normalized dry thickness of brushes (a) S₃ and (b) S₇ as a function of the incubation time in pH 3 and 10 solutions.

mean-square (RMS) roughness calculated from each of these images is given below the height images. Brushes displayed similar morphologies in buffer solutions, although a significant increase observed in RMS for S₇, when incubated at pH 10. Height profiles, which were used to determine swelling ratios, are presented in Figures S11 and S12. Brushes exhibited lower swelling ratios in buffer solutions compared to values

determined in DIW, due to the screened charges and reduced electrostatic interactions. No drastic change is observed in swelling behavior, which indicates that the degree of charging does not depend on pH at 64% of DQ, and brushes behave as strong polyelectrolytes.

In solution AFM analyses proved that it is possible to obtain PEBs with good hydration properties, by combining hydro-

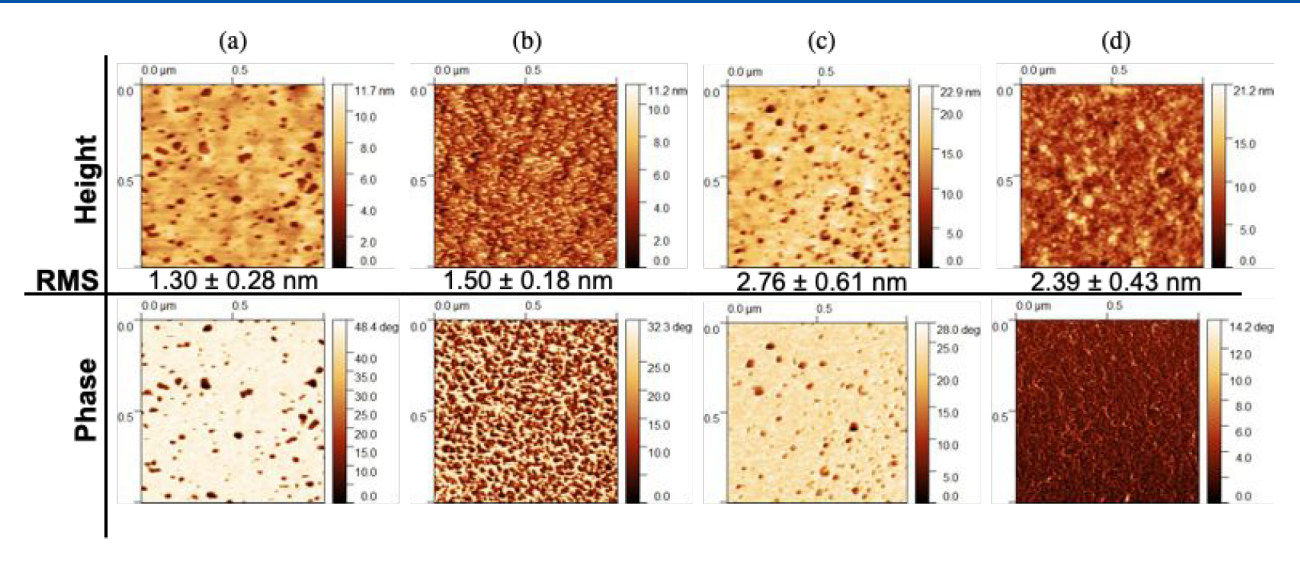


Figure 7. AFM images $(1 \mu m \times 1 \mu m)$ of samples after 3 weeks of incubation. (a) S_3 in pH 3, (b) S_3 in pH 10, (c) S_7 in pH 3, (d) S_7 in pH 10.

phobic and ionic units in an alternating sequence. To elucidate the role of macromolecular architecture and composition in brush stability, brushes were incubated in buffer solutions (pH 3 and 10) for 3 weeks. Samples were removed from the solution at certain time intervals, rinsed with DIW, and dried under a vacuum, then the dry thickness was measured via AFM. The dry thickness of polymer brushes (h) is defined by the molecular weight (MW) and grafting density σ_i , i.e., h = $(MW \cdot \sigma)/(\rho \cdot NA)$, where ρ is polymer density and NA is Avogadro's number. Therefore, a decrease in brush height can be explained by the change of either MW or σ . The MW of the brushes should remain constant, since the poly(styrene-alt-Nmaleimide) backbone is expected to be chemically stable under incubation conditions.⁵¹ Whereas, the grafting density might decrease by the detachment of the brushes from the substrate. Figure 6a and b show the normalized thickness of brushes as a function of incubation time and pH. Sample S₃, which bears an ethylenediamine-based spacer, retains more than 80% of the brush height after 21 days in buffer solutions. In addition, the extent of degrafting is nearly identical for acidic or basic mediums. A similar trend was reported in the literature where it is attributed to the lack of hydrolysis vulnerable groups such as ester functions. 32,52 However, the sample with an oligoethylene oxide based spacer (S₇) exhibited different degrafting kinetics with varying pH. After a total incubation time of 21 days, the sample incubated at pH 3 preserves ~92% of the initial height, which is ~12% higher than that at pH 10. This trend can be explained by the effect of increased tension due to enhanced hydrophilicity and steric effects of bulkier side chains, which accelerate degrafting combined with basecatalyzed hydrolysis at high concentration of the hydroxide ions in pH 10. Control experiments were conducted at pH 7 to confirm the data obtained from incubation tests at pH 3 and 10. Samples were incubated at pH 7 for 6 days, and dry thicknesses were measured every 48 h. Similar trends were observed for both S3 and S7, which retained 89% and 90% of their initial thicknesses (Figure S13), respectively.

To provide a comparison with homopolymer based systems, PMETAC brushes (h_0 : 21.1 nm) (Figure S14), which are strong cationic polyelectrolytes (DQ 100%) with a methacrylate-based backbone and similar swelling properties ($h_{\rm DIW}/h_0$: 3.1), were synthesized and evaluated under identical conditions. Figure S15 presents the variation of normalized

thickness of PMETAC brushes within 6 days of incubation. PMETAC brushes exhibited limited stability, displaying a significant reduction (~69%) in normalized thickness of the sample incubated at pH 10 during that time, whereas the sample retained ~51% of its initial height at pH 3 over that same period. After 3 weeks of incubation, alternating copolymer brushes retained more than 80% of their original height and revealed higher stability compared to homopolymer strong cationic brushes. Our findings suggest that the distribution of the charges along with the side chain chemistry plays an important role in stability and swelling behavior of the brushes. Alternating sequences of neutral and charged segments as well as separating the charge from the backbone contributed to stability by reducing the charge density along the polymer chain. A more detailed study is required to understand the precise role of the pendant chains bearing the charged groups in swelling properties and overall stability of the brushes.

Figure 7 shows the AFM surface height and phase images of brushes before and after incubation. Surface roughness values were determined from the height images with a scan size 1×1 μ m². Samples S₃ and S₇ exhibited similar morphologies in the dry state, with relatively uniform phase images and RMS roughness values of 0.7 and 0.61, respectively (Figure 5). For both samples, an increase in RMS roughness was observed after incubation, accompanied by the changes in surface morphology which strongly depend on the pH. Samples incubated at pH 3 displayed perforated top layers with pinholelike structures. The contrast in the phase images also confirms the formation of heterogeneous layers having different stiffness from the underlying polymer. Resulting morphologies can be associated with the different solubility behavior of charged and neutral units. Long-term exposure of the brushes to aqueous buffer solutions, which represent poor solvent conditions for hydrophobic styrene units, may induce rearrangement of the brushes. To support this claim control experiments were conducted with homopolymer polystyrene (PS) brushes. PS brushes with a 20 nm height were incubated in buffer solutions and then characterized with AFM. After 72 h of incubation, similar features appeared on the surface of PS brushes; no significant change was determined in the brush height (Figure S16). Samples incubated at pH 10 adopted different morphologies, with no evident pattern. The difference between

the morphologies at varying pH might be related to the pH-mediated hydroxide adsorption to the brushes, which creates interchain hydrogen bonds and physical cross-links, resulting in stiffer brushes with restricted mobility at increasing pH. ⁵³

CONCLUSION

In summary, a series of strong cationic PEBs were synthesized through alternating copolymerization of styrene and tailormade charge-bearing N-substituted maleimides and evaluated in terms of swelling behavior and stability in various environments. The stability data, collected over a 3 week incubation period at two different pH's, showed that introduction of hydrophobic-neutral units to reduce the number of charged group monomers along the backbone is an effective strategy. Uniform distribution of charges in an alternating sequence enabled the obtainment of brushes with good hydration properties and contributed to stability by lowering Coulombic stress. We demonstrated that the composition of the tailored side arms also plays an important role in the brush performance; using oligo(ethylene oxide) alkyl-based spacers instead of short alkyl chains enhances the hydration behavior without diminishing stability. Outcomes of this study provide important insights into the design of stable brush systems with a novel approach.

ASSOCIATED CONTENT

Supporting Information

The Supporting Information is available free of charge at https://pubs.acs.org/doi/10.1021/acs.macromol.2c00647.

¹H NMR spectra of Mono-Boc protected diamines, monomers, and polymers; XPS survey spectra of initiator immobilized substrates and quaternized brushes; water contact angles of initiator immobilized substrates and PS brushes; AFM height and phase images of PEBs and PS brushes; stability data of PMETAC brushes (PDF)

AUTHOR INFORMATION

Corresponding Author

Christopher K. Ober – Materials Science and Engineering, Cornell University, Ithaca, New York 14853, United States; oorcid.org/0000-0002-3805-3314; Email: cko3@cornell.edu

Author

Gozde Aktas Eken – Materials Science and Engineering, Cornell University, Ithaca, New York 14853, United States

Complete contact information is available at: https://pubs.acs.org/10.1021/acs.macromol.2c00647

Funding

This work is supported by the National Science Foundation (CHE 2003588).

Notes

The authors declare no competing financial interest.

ACKNOWLEDGMENTS

This study was primarily supported by the National Science Foundation through grant NSF CHE 200358. The authors would also like to acknowledge the Center for Research on Programmable Plant System (CROPPS) for the financial support with major support from the National Science

Foundation under grant no. DBI 2019674. This work made use of the Cornell Center for Materials Research Shared Facilities, which is supported through the NSF MRSEC program (DMR-1719875) and CESI Shared Facilities partly sponsored by the NSF MRI DMR-1338010 and Kavli Institute at Cornell (KIC). This work made use of the Cornell NMR Facility, which was supported, in part, by the NSF through MRI award CHE-1531632.

REFERENCES

- (1) Chen, W.-L.; Cordero, R.; Tran, H.; Ober, C. K. 50th Anniversary Perspective: Polymer Brushes: Novel Surfaces for Future Materials. *Macromolecules* **2017**, *50* (11), 4089–4113.
- (2) Zoppe, J. O.; Ataman, N. C.; Mocny, P.; Wang, J.; Moraes, J.; Klok, H.-A. Surface-Initiated Controlled Radical Polymerization: State-of-the-Art, Opportunities, and Challenges in Surface and Interface Engineering with Polymer Brushes. *Chem. Rev.* **2017**, *117* (3), 1105–1318.
- (3) Zhao, B.; Brittain, W. J. Polymer brushes: surface-immobilized macromolecules. *Prog. Polym. Sci.* **2000**, *25* (5), *677*–710.
- (4) Buhl, K. B.; Møller, R. K.; Heide-Jørgensen, S.; Kolding, A. N.; Kongsfelt, M.; Budzik, M. K.; Hinge, M.; Pedersen, S. U.; Daasbjerg, K. Highly Efficient Rubber-to-Stainless Steel Bonding by Nanometer-Thin Cross-linked Polymer Brushes. *ACS Omega* **2018**, 3 (12), 17511–17519.
- (5) Yan, J. J.; Bockstaller, M. R.; Matyjaszewski, K. Brush-modified materials: Control of molecular architecture, assembly behavior, properties and applications. *Prog. Polym. Sci.* **2020**, *100*, 101180.
- (6) Ma, S.; Zhang, X.; Yu, B.; Zhou, F. Brushing up functional materials. NPG Asia Materials 2019, 11 (1), 24.
- (7) Xie, Z.; Gan, T.; Fang, L.; Zhou, X. Recent progress in creating complex and multiplexed surface-grafted macromolecular architectures. *Soft Matter* **2020**, *16* (38), 8736–8759.
- (8) Ballauff, M.; Borisov, O. Polyelectrolyte brushes. Curr. Opin. Colloid Interface Sci. 2006, 11 (6), 316–323.
- (9) Das, S.; Banik, M.; Chen, G.; Sinha, S.; Mukherjee, R. Polyelectrolyte brushes: theory, modelling, synthesis and applications. *Soft Matter* **2015**, *11* (44), 8550–8583.
- (10) Xu, X.; Billing, M.; Ruths, M.; Klok, H.-A.; Yu, J. Structure and Functionality of Polyelectrolyte Brushes: A Surface Force Perspective. *Chemistry An Asian Journal* **2018**, *13* (22), 3411–3436.
- (11) Farhan, T.; Azzaroni, O.; Huck, W. T. S. AFM study of cationically charged polymer brushes: switching between soft and hard matter. *Soft Matter* **2005**, *1* (1), 66–68.
- (12) Moro, T.; Takatori, Y.; Ishihara, K.; Konno, T.; Takigawa, Y.; Matsushita, T.; Chung, U.-i.; Nakamura, K.; Kawaguchi, H. Surface grafting of artificial joints with a biocompatible polymer for preventing periprosthetic osteolysis. *Nat. Mater.* **2004**, 3 (11), 829–836.
- (13) Ferrand-Drake del Castillo, G.; Koenig, M.; Müller, M.; Eichhorn, K.-J.; Stamm, M.; Uhlmann, P.; Dahlin, A. Enzyme Immobilization in Polyelectrolyte Brushes: High Loading and Enhanced Activity Compared to Monolayers. *Langmuir* **2019**, 35 (9), 3479–3489.
- (14) Yang, Q.; Li, L.; Sun, L.; Ye, Z.; Wang, Y.; Guo, X. Spherical polyelectrolyte brushes as bio-platforms to integrate platinum nanozyme and glucose oxidase for colorimetric detection of glucose. *J. Polym. Sci.* **2021**, *59* (19), 2201–2211.
- (15) Li, B.; Du, T.; Yu, B.; van der Gucht, J.; Zhou, F. Caterpillar-Inspired Design and Fabrication of A Self-Walking Actuator with Anisotropy, Gradient, and Instant Response. *Small* **2015**, *11* (28), 3494–3501.
- (16) Zhou, F.; Shu, W.; Welland, M. E.; Huck, W. T. S. Highly Reversible and Multi-Stage Cantilever Actuation Driven by Polyelectrolyte Brushes. *J. Am. Chem. Soc.* **2006**, *128* (16), 5326–5327.
- (17) Li, M.; Pester, C. W. Mixed Polymer Brushes for "Smart" Surfaces. *Polymers (Basel)* **2020**, *12* (7), 1553.

- (18) Higaki, Y.; Nishida, J.; Takenaka, A.; Yoshimatsu, R.; Kobayashi, M.; Takahara, A. Versatile inhibition of marine organism settlement by zwitterionic polymer brushes. *Polym. J.* **2015**, *47* (12), 811–818.
- (19) Guo, S.; Quintana, R.; Cirelli, M.; Toa, Z. S. D.; Arjunan Vasantha, V.; Kooij, E. S.; Jańczewski, D.; Vancso, G. J. Brush Swelling and Attachment Strength of Barnacle Adhesion Protein on Zwitterionic Polymer Films as a Function of Macromolecular Structure. Langmuir: the ACS journal of surfaces and colloids 2019, 35 (24), 8085–8094.
- (20) Fromel, M.; Sweeder, D. M.; Jang, S.; Williams, T. A.; Kim, S. H.; Pester, C. W. Superhydrophilic Polymer Brushes with High Durability and Anti-fogging Activity. *ACS Applied Polymer Materials* **2021**, 3 (10), 5291–5301.
- (21) Daniel, D.; Goh, S. S.; Truong, T. N. B.; Koh, X. Q.; Tomczak, N. Origin of Underwater Oil-Repellence in Polyelectrolyte Brush Surfaces. *Advanced Materials Interfaces* **2021**, 8 (2), 2001203.
- (22) Kumar Vyas, M.; Schneider, K.; Nandan, B.; Stamm, M. Switching of friction by binary polymer brushes. *Soft Matter* **2008**, *4* (5), 1024–1032.
- (23) Wei, Q.; Cai, M.; Zhou, F.; Liu, W. Dramatically Tuning Friction Using Responsive Polyelectrolyte Brushes. *Macromolecules* **2013**, *46* (23), 9368–9379.
- (24) Chen, L.; Xie, Z.; Gan, T.; Wang, Y.; Zhang, G.; Mirkin, C. A.; Zheng, Z. Biomimicking Nano-Micro Binary Polymer Brushes for Smart Cell Orientation and Adhesion Control. *Small* **2016**, *12* (25), 3400–3406.
- (25) Klok, H.-A.; Genzer, J. Expanding the Polymer Mechanochemistry Toolbox through Surface-Initiated Polymerization. *ACS Macro Lett.* **2015**, *4* (6), 636–639.
- (26) Tugulu, S.; Klok, H.-A. Stability and Nonfouling Properties of Poly(poly(ethylene glycol) methacrylate) Brushes under Cell Culture Conditions. *Biomacromolecules* **2008**, *9* (3), 906–912.
- (27) Melzak, K. A.; Yu, K.; Bo, D.; Kizhakkedathu, J. N.; Toca-Herrera, J. L. Chain Length and Grafting Density Dependent Enhancement in the Hydrolysis of Ester-Linked Polymer Brushes. *Langmuir* **2015**, *31* (23), 6463–6470.
- (28) Borozenko, O.; Ou, C.; Skene, W. G.; Giasson, S. Polystyrene-block-poly(acrylic acid) brushes grafted from silica surfaces: pH- and salt-dependent switching studies. *Polym. Chem.* **2014**, 5 (7), 2242–2252.
- (29) Patil, R.; Miles, J.; Ko, Y.; Datta, P.; Rao, B. M.; Kiserow, D.; Genzer, J. Kinetic Study of Degrafting Poly(methyl methacrylate) Brushes from Flat Substrates by Tetrabutylammonium Fluoride. *Macromolecules* **2018**, *51* (24), 10237–10245.
- (30) Wang, J.; Klok, H.-A. Swelling-Induced Chain Stretching Enhances Hydrolytic Degrafting of Hydrophobic Polymer Brushes in Organic Media. *Angew. Chem., Int. Ed.* **2019**, 58 (29), 9989–9993.
- (31) Borozenko, O.; Godin, R.; Lau, K. L.; Mah, W.; Cosa, G.; Skene, W. G.; Giasson, S. Monitoring in Real-Time the Degrafting of Covalently Attached Fluorescent Polymer Brushes Grafted to Silica Substrates—Effects of pH and Salt. *Macromolecules* **2011**, *44* (20), 8177–8184.
- (32) Chen, W.-L.; Menzel, M.; Watanabe, T.; Prucker, O.; Rühe, J.; Ober, C. Reduced Lateral Confinement and Its Effect on Stability in Patterned Strong Polyelectrolyte Brushes. *Langmuir* **2017**, *33*, 3296.
- (33) Ko, Y.; Genzer, J. Spontaneous Degrafting of Weak and Strong Polycationic Brushes in Aqueous Buffer Solutions. *Macromolecules* **2019**, 52 (16), 6192–6200.
- (34) Menzel, M.; Chen, W.-L.; Simancas, K.; Xu, H.; Prucker, O.; Ober, C. K.; Rühe, J. Entropic death of nonpatterned and nanopatterned polyelectrolyte brushes. *J. Polym. Sci., Part A: Polym. Chem.* **2019**, *57* (12), 1283–1295.
- (35) Galvin, C. J.; Bain, E. D.; Henke, A.; Genzer, J. Instability of Surface-Grafted Weak Polyacid Brushes on Flat Substrates. *Macromolecules* **2015**, 48 (16), 5677–5687.
- (36) Ataman, N. C.; Klok, H.-A. Degrafting of Poly(poly(ethylene glycol) methacrylate) Brushes from Planar and Spherical Silicon Substrates. *Macromolecules* **2016**, 49 (23), 9035–9047.

- (37) Quintana, R.; Gosa, M.; Jańczewski, D.; Kutnyanszky, E.; Vancso, G. J. Enhanced Stability of Low Fouling Zwitterionic Polymer Brushes in Seawater with Diblock Architecture. *Langmuir* **2013**, 29 (34), 10859–10867.
- (38) Li, Y.; Ko, Y.; Lin, Y.; Kiserow, D.; Genzer, J. Enhanced Stability of Surface-Tethered Diblock Copolymer Brushes with a Neutral Polymer Block and a Weak Polyelectrolyte Block: Effects of Molecular Weight and Hydrophobicity of the Neutral Block. *Macromolecules* **2017**, *50* (21), 8580–8587.
- (39) Pfeifer, S.; Lutz, J.-F. Development of a Library of N-Substituted Maleimides for the Local Functionalization of Linear Polymer Chains. *Chem.—Eur. J.* **2008**, *14* (35), 10949–10957.
- (40) Lutz, J.-F.; Schmidt, B. V. K. J.; Pfeifer, S. Tailored Polymer Microstructures Prepared by Atom Transfer Radical Copolymerization of Styrene and N-substituted Maleimides. *Macromol. Rapid Commun.* **2011**, 32 (2), 127–135.
- (41) Chen, F. C. M.; Benoiton, N. L. A new method of quaternizing amines and its use in amino acid and peptide chemistry. *Can. J. Chem.* 1976, 54 (20), 3310–3311.
- (42) Zhang, T.; Du, Y.; Kalbacova, J.; Schubel, R.; Rodriguez, R. D.; Chen, T.; Zahn, D. R. T.; Jordan, R. Wafer-scale synthesis of defined polymer brushes under ambient conditions. *Polym. Chem.* **2015**, *6* (47), 8176–8183.
- (43) Zhang, T.; Du, Y.; Müller, F.; Amin, I.; Jordan, R. Surface-initiated Cu(0) mediated controlled radical polymerization (SI-CuCRP) using a copper plate. *Polym. Chem.* **2015**, *6* (14), 2726–2733
- (44) Patil, R. R.; Turgman-Cohen, S.; Šrogl, J.; Kiserow, D.; Genzer, J. Direct Measurement of Molecular Weight and Grafting Density by Controlled and Quantitative Degrafting of Surface-Anchored Polymethyl methacrylate). ACS Macro Lett. 2015, 4 (2), 251–254.
- (45) Terada, S.; Matsumoto, A. Role of N-substituents of maleimides on penultimate unit effect for sequence control during radical copolymerization. *Polym. J.* **2019**, *51* (11), 1137–1146.
- (46) Nishimori, K.; Sawamoto, M.; Ouchi, M. Design of maleimide monomer for higher level of alternating sequence in radical copolymerization with styrene. *J. Polym. Sci., Part A: Polym. Chem.* **2019**, *57* (3), 367–375.
- (47) Lee, H. J.; Jamison, A. C.; Lee, T. R. Boc-Protected ω -Amino Alkanedithiols Provide Chemically and Thermally Stable Amine-Terminated Monolayers on Gold. *Langmuir* **2015**, *31* (7), 2136—2146.
- (48) Malinowski, S.; Jaroszyńska-Wolińska, J.; Herbert, P. Theoretical insight into plasma deposition of laccase bio-coating formation. *J. Mater. Sci.* **2019**, *54*, 10746.
- (49) Koufakis, E.; Manouras, T.; Anastasiadis, S. H.; Vamvakaki, M. Film Properties and Antimicrobial Efficacy of Quaternized PDMAE-MA Brushes: Short vs Long Alkyl Chain Length. *Langmuir* **2020**, *36* (13), 3482–3493.
- (50) Cheng, N.; Bao, P.; Evans, S. D.; Leggett, G. J.; Armes, S. P. Facile Formation of Highly Mobile Supported Lipid Bilayers on Surface-Quaternized pH-Responsive Polymer Brushes. *Macromolecules* **2015**, *48* (9), 3095–3103.
- (51) Suwier, D. R.; Steeman, P. A. M.; Teerenstra, M. N.; Schellekens, M. A. J.; Vanhaecht, B.; Monteiro, M. J.; Koning, C. E. Flexibilized Styrene-N-Substituted Maleimide Copolymers with Enhanced Entanglement Density. *Macromolecules* **2002**, *35* (16), 6210–6216.
- (52) Bain, E. D.; Dawes, K.; Özçam, A. E.; Hu, X.; Gorman, C. B.; Šrogl, J.; Genzer, J. Surface-Initiated Polymerization by Means of Novel, Stable, Non-Ester-Based Radical Initiator. *Macromolecules* **2012**, *45* (9), 3802–3815.
- (53) Wu, B.; Wang, X.; Yang, J.; Hua, Z.; Tian, K.; Kou, R.; Zhang, J.; Ye, S.; Luo, Y.; Craig, V. S. J.; Zhang, G.; Liu, G. Reorganization of hydrogen bond network makes strong polyelectrolyte brushes pHresponsive. *Science Advances* **2016**, *2* (8), No. e1600579.